

SUPPORTING INFORMATION

Quench ionic Flash NanoPrecipitation (qiFNP) as a simple and tunable approach to decouple growth and functionalization for the one-step synthesis of functional LnPO₄-based nanoparticle in water

Nathalie M PINKERTON,^[a] Khadidja HADRI,^[a,c] Baptiste AMOUROUX,^[c] Leah BEHAR,^[b]
Christophe MINGOTAUD,^[c] Mathias DESTARAC,^[c] Ihor KULAI,^[c] Stéphane MAZIERES,^[c]
Stefan CHASSAING^{[a,d]*} & Jean-Daniel MARTY^{[c]*}

*[a] ITAV, Université de Toulouse, CNRS USR3505, UPS
1 place Pierre Potier, 31106 Toulouse Cedex 1 (France)*

*[b] Department of Chemistry, Mars Hill University
Mars Hill, NC 28754 (United States)*

*[c] IMRCP, Université de Toulouse, CNRS UMR5623, UPS
118 route de Narbonne, 31062 Toulouse Cedex 1 (France)
marty@chimie.ups-tlse.fr

*[d] Laboratoire de Synthèse et Réactivités Organiques & Catalyse,
Institut de Chimie de Strasbourg, CNRS UMR7177
4 rue Blaise Pascal, 67070 Strasbourg (France)
chassaing@unistra.fr

Contents:

Acronyms	S3
General	S4
General experimental procedures	S7
PEGylated Gadolinium Phosphate Nanoparticle Characterization	S8
PEGylated Europium Phosphate Nanoparticle Characterization	S9
PEGylated Mixed Lanthanide Phosphate Nanoparticle Characterization	S11
Polymer – Synthesis & Characterization	S14
PEGylated Fluorescent Nanoparticle Characterization	S20
References	S21

Acronyms:

AA	Acrylic Acid
AIBN	Azobisobutyronitrile
BCP	Block Copolymer
DLS	Dynamic Light Scattering
DMAAm	<i>N,N</i>-Dimethylacrylamide
EtOAc	Ethyl Acetate
Eu	Europium
EuPO₄	Europium Phosphate
ICP	Inductively Coupled Plasma
iFNP	ionic Flash NanoPrecipitation
FNP	Flash NanoPrecipitation
Gd	Gadolinium
GdPO₄	Gadolinium Phosphate
LnPO₄	Lanthanide Phosphate
MR	Magnetic Resonance
MRI	Magnetic Resonance Imaging
NMR	Nuclear Magnetic Resonance
NP	Nanoparticle
PAA	Poly(Acrylic Acid)
PAA-PDMAAm-C	Poly(Acrylic Acid)-<i>b</i>-Poly(Dimethyl Acrylamide)-Coumarin
PAA-PEG	Poly(Acrylic Acid)-<i>b</i>-Poly(Ethylene Glycol)
PBS	Phosphate Buffered Saline
qiFNP	quench ionic Flash NanoPrecipitation
TEM	Transmission Electron Microscopy
THF	Tetrahydrofuran
XRD	X-Ray Diffraction
ZP	Zeta Potential

General

A. Materials

PAA-PEG 3k-*b*-6k was purchased from Polymer Source, Inc. Acrylic acid (99%, Sigma-Aldrich), sodium chloride (Sigma-Aldrich), sodium phosphate monobasic (Sigma-Aldrich), sodium hydroxide (Sigma-Aldrich), hydrochloric acid (Sigma-Aldrich or Alfa Aesar), Tris buffer (Sigma-Aldrich), gadolinium (III) nitrate hexahydrate (Sigma-Aldrich), europium (III) chloride hexahydrate (Alfa Aesar), 2-bromopropionyl bromide (Alfa Aesar), 4-*N,N*-(diethylamino)salicylaldehyde (Alfa Aesar), 4-nitrophenylacetonitrile (Alfa Aesar), piperidine (Alfa Aesar), potassium ethyl xanthogenate (Sigma-Aldrich), tin(II) chloride dihydrate (Alfa Aesar) and triethylamine (Sigma-Aldrich) were commercial and were used as received. 2-Bromo-*N*-(4-(7-(diethylamino)-2-oxo-2H-chromen-3-yl)phen-yl)propanamide was prepared according to the method reported by Kulai & Mallet-Ladeira.¹ *N,N*-dimethylacrylamide (DMAAm, Sigma-Aldrich) and acrylic acid (AA, Sigma-Aldrich) were passed through a column filled with neutral aluminium oxide (Brockmann I) prior to use. 2,2'-Azobis(2-methylpropionitrile) (AIBN, Acros) was purified by double recrystallization from methanol. The *O*-ethyl-*S*-(1-methoxycarbonyl) ethyldithiocarbonate MADIX agent (Rhodixan A1) was obtained from Rhodia and used as received. The 4,4'-Azobis(4-cyanovaleric acid) initiator (>98%, ACVA) was purchased from Janssen Chimica and recrystallized from ethanol before use. Bovine serum albumin was purchased from Euromedex. Organic solvents were received from Sigma-Aldrich and used without additional purification. Ultra-pure water (18.2 MΩ·cm) was generated using a ELGA Purelab® Ultra purification system. PAA-PEG solutions were titrated to a pH of 5.2 using 2M NaOH. All aqueous solutions were filtered with a 0.22 μm regenerated cellulose syringe filter (Agela Technologies) to remove dust prior to nanoparticle formation.

B. Methods

B.1. Nanoparticle characterization – NP size was determined *via* DLS using a Zetasizer Nano-ZS (Malvern Instruments, France). The reported particle size is the intensity weighted diameter determined by the Malvern deconvolution software in normal mode. – ZP measurements were done on NPs in a 3 mM NaCl solution using the aforementioned

Zetasizer Nano-ZS. – TEM samples deposited on holey carbon grids and imaged on a Hitachi HT-7700. TEM images were analyzed with ImageJ. – XRD samples were dialyzed against ultra-pure water using a Spectra/Por® regenerated cellulose membrane (MWCO 6-8 kD) and then lyophilized (Christ Alpha 2-4 LD lyophilizer, Germany). Powder XRD spectra of the dried powders were recorded on an MPDPro diffractometer (PANalytical B.V.) (Cu K α source) from 2° to 90° (2 θ) with a step size of 0.017°. – Steady state absorption and emission spectra were made using a Xenius Fluorometer (SAFAS, Monaco) and a Fluoroskan Ascent Microplate Fluorometer (Thermo Fisher, France), or a Horiba Jobin Yvon Fluoromax-4 spectrofluorometer equipped with a xenon lamp. – For ICP measurements, nanoparticle samples were digested in nitric acid for 1 day, and then analyzed using a Perkin Elmer Optima 3200 RL (USA). – MR relaxation time measurements were carried out at 1.4 T on a Minispec mq60 TD-NMR contrast agent analyzer (Bruker Optics, Billerica, MA, USA) at a constant temperature of 37 °C. T₁ relaxation times were measured using an inversion recovery pulse sequence (t1_ir_mb). T₂ relaxation times were measured using a Carr–Purcell–Meiboom–Gill pulse sequence (t2_cp_mb).

B.2. Organic synthesis – The reactions were monitored by thin-layer chromatography carried out on silica plates (silica gel 60 F254, Merck) using UV-light for visualization. Column chromatographies were performed on 35-70 μ m silica gel 60 (porosity 90 Å) using the indicated mixture of solvents as eluent. – Evaporation of solvents were conducted under reduced pressure at temperatures less than 30°C unless otherwise noted. – IR spectra were recorded using a Thermo Fischer Nexus 6700 FTIR spectrometer in ATR mode. Values are reported in cm⁻¹. – ¹H and ¹³C NMR spectra were recorded on a Bruker Avance 300 spectrometer at 300 and 75 MHz, respectively. Chemical shifts δ and coupling constants J are given in ppm and Hz, respectively. Chemical shifts δ are reported relative to residual solvent as an internal standard (*e.g.* for CDCl₃, 7.26 ppm and 77.0 ppm for ¹H for ¹³C NMR, respectively). The splitting abbreviations are : s = singlet, d = doublet, t = triplet and q = quadruplet. – Electrospray (ESI) high-resolution mass spectra (HRMS) were measured on Waters GCT Premier CAB109 TOF detector from the 'Service Commun de Spectroscopie de Masse' of the Plateforme Technique, Institut de Chimie de Toulouse.

B.3. Polymer characterization – The monomer conversions were determined by ¹H NMR and the number-average molar mass (M_n) and dispersity (\mathcal{D}) values for the prepared

polymer samples were obtained from size-exclusion chromatography (SEC). The SEC analyses were conducted on a system composed of Waters 515 HPLC pump, Waters 717plus autosampler, set of two Shodex columns (OHpak SB-806 M HQ, 13 μm , 8.0 mm \times 300 mm and OHpak SB-802.5 HQ, 13 μm , 8.0 mm \times 300 mm), Varian ProStar 325 UV-Vis detector set at 290 nm, Wyatt DAWN Heleos Multi-Angle Light Scattering (MALS) detector and Shodex RI-101 differential refractive index detector. Phosphate-buffered saline (NaCl 100 mmol L⁻¹, NaH₂PO₄ 25 mmol L⁻¹, Na₂HPO₄ 25 mmol L⁻¹, pH = 7) was used as eluent with a flow rate of 1.0 mL min⁻¹. Prior to injection, samples were diluted to a concentration of 5 mg mL⁻¹ and filtered through 0.45 mm cellulose acetate syringe filters. – The dn/dc values were measured using a PSS DnDc-2010 differential refractometer (λ = 620 nm, 35 °C). Series of polymer solutions with concentrations from 0.5 to 10 mg mL⁻¹ were used.

General experimental procedures

A. Nanoparticle Formation

Nanoparticles were formed *via* quench ionic Flash NanoPrecipitation (*qiFNP*) using a confined impinging jet (CIJ) mixer designed by Han *et al.*² As an example formulation, water stream 1 containing 1 mg/mL NaH₂PO₄ was rapidly mixed against water stream 2 containing 5.2 mg/mL Gd(NO₃)₃ using the CIJ mixer. The output stream was injected into a stirring (1000 rpm, IKA) 10 mg/ml PAA-*b*-PEG 3k-*b*-6k solution in water. Equal volumes of streams 1, 2 and the quench were used. Particles were dialyzed against ultra-pure water using a Spectra/Por® regenerated cellulose membrane (MWCO 6-8 kD).

B. Nanoparticle Stability Testing

The stability of the nanoparticles overtime under storage and physiological conditions was tested. Particles were stored at 4°C in the dark post *qiFNP* formation. Their stability was monitored over the course of six days visually and *via* DLS. For biologically-relevant conditions, particles were incubated in Tris buffer (pH 7.4) with 3 wt% albumin and periodically monitored visually and *via* DLS over the course of 24 hours. To distinguish both the albumin (6 to 7 nm) and the NP populations (40 nm), the intensity weighted diameters were determined by the Malvern deconvolution software in high resolution mode (multiple narrow modes).

PEGylated Gadolinium Phosphate Nanoparticle Characterization

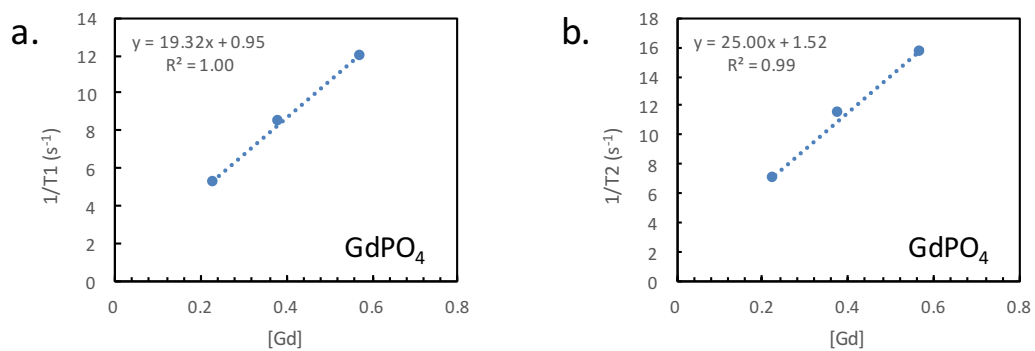
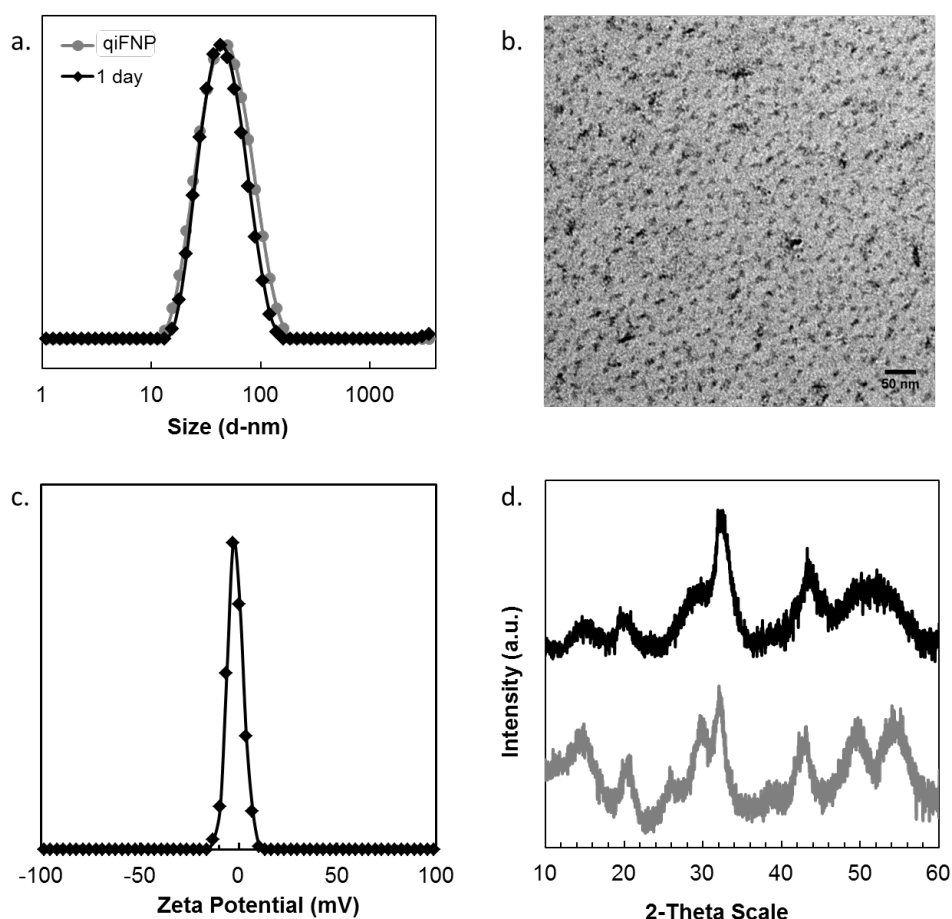


Figure S1. Plots of T1 relaxation rates (a) and T2 relaxation rates (b) for 50 nm GdPO₄ nanoparticles.

PEGylated Europium Phosphate Nanoparticle Characterization

As mentioned in the main text, the qiFNP process is flexible. The nature of the nanoparticle core can be simply changed by substituting one lanthanide for another. In this example, the Gd is substituted with Eu to form PEGylated luminescent EuPO_4 nanoparticles. The EuPO_4 nanoparticles have an intensity weighted size of 50 nm (PDI = 0.19) and a zeta potential of -2.2 ± 1.0 mV (**Figures S2a,c**). The particles are very stable in both storage conditions at 4°C and in albumin-rich, physiologically relevant conditions over 24 hours (**Figures S2a and S3**). The near neutral zeta potential and the particle stability in the presence of albumin suggest a high PEG density. Moreover, smaller 40 nm-sized NPs can be obtained under more dilute lanthanide conditions with a large excess of $\text{PAA}_{3k}\text{-}b\text{-PEG}_{6k}$ polymer (**Figures S2e**).



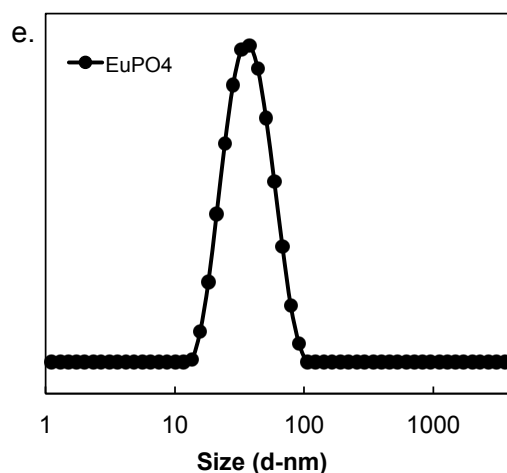


Figure S2. (a.) The intensity weighted size of EuPO_4 nanoparticles after qiFNP formation and after 1-day in storage conditions. The particles have an average size of 50 nm (PDI = 0.19). (b.) The TEM image of the nanoparticles. Only the inorganic core has sufficient electron density contrast to be observed. The cores are very homogeneous in size. (c.) The zeta potential plot of the nanoparticles. The particles have a near neutral zeta potential of -2.2 ± 1.0 mV. (d.) The XRD traces of the EuPO_4 nanoparticles and the EuPO_4 salt. The characteristic EuPO_4 peaks are observed in the NP sample. (e.) The intensity weighted size of EuPO_4 nanoparticles after qiFNP formation under more dilute lanthanide conditions. The particles have an average size of 40 nm (PDI = 0.24) (reaction conditions – 5 mg/mL PAA-PEG, 4.2 mg/mL $\text{EuCl}_3 \cdot 6\text{H}_2\text{O}$ and 1 mg/ml NaH_2PO_4).

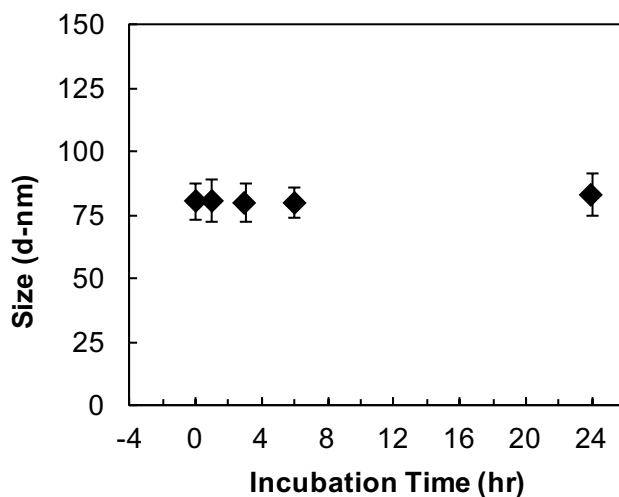


Figure S3. The intensity weighted size of EuPO_4 nanoparticles incubated in physiological relevant media. The particle size remains at 80 ± 7 nm over the course of the 24 hr incubation period (n=3).

PEGylated Mixed Lanthanide Phosphate Nanoparticle Characterization

To form multi-modal nanoparticles for both fluorescence and MR imaging, both Gd and Eu can be incorporated into the nanoparticles. In terms of size and stability, the mixed lanthanide nanoparticles have similar properties to the single lanthanide nanoparticles. As shown in **Figure S4a**, the nanoparticles have an intensity weighted size of 48 nm (PDI = 0.21). The uniform cores can be observed *via* TEM (**Figure S4b**). The particles are also highly PEGylated with a near neutral zeta potential of -2.0 ± 1.0 mV (**Figure S4c**). As a result, they are stable in physiologically relevant media (**Figure S4d**). The Gd to Eu ratio can be used to tune the nanoparticle properties. As described in the main text, the ratio affects the relaxivity of the particle. The ratio also affects the fluorescence of the nanoparticle (**Figure S5d**). The fluorescence intensity increases linearly with the Eu content.

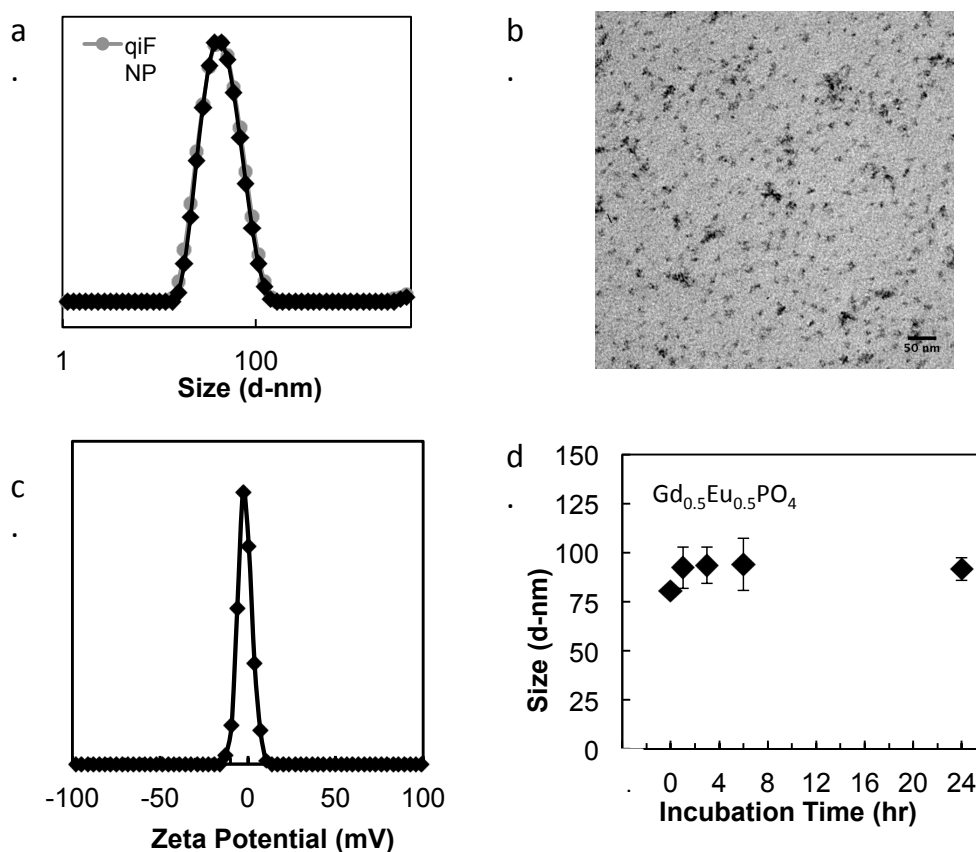


Figure S4. (a.) The intensity weighted size of $Gd_{0.5}Eu_{0.5}PO_4$ nanoparticles after qiFNP formation and after 1-day in storage conditions. The particles have an average size of 48 nm (PDI = 0.21). (b.) The TEM image of the nanoparticles. Only the inorganic core has sufficient electron density contrast to be observed. (c.) The zeta potential plot of the nanoparticles. The particles have a near neutral zeta potential of -2.0 ± 1.0 mV. (d.) The intensity weighted size of $Gd_{0.5}Eu_{0.5}PO_4$ nanoparticles incubated in physiological relevant media over the course of the 24 hr incubation period (n=3).

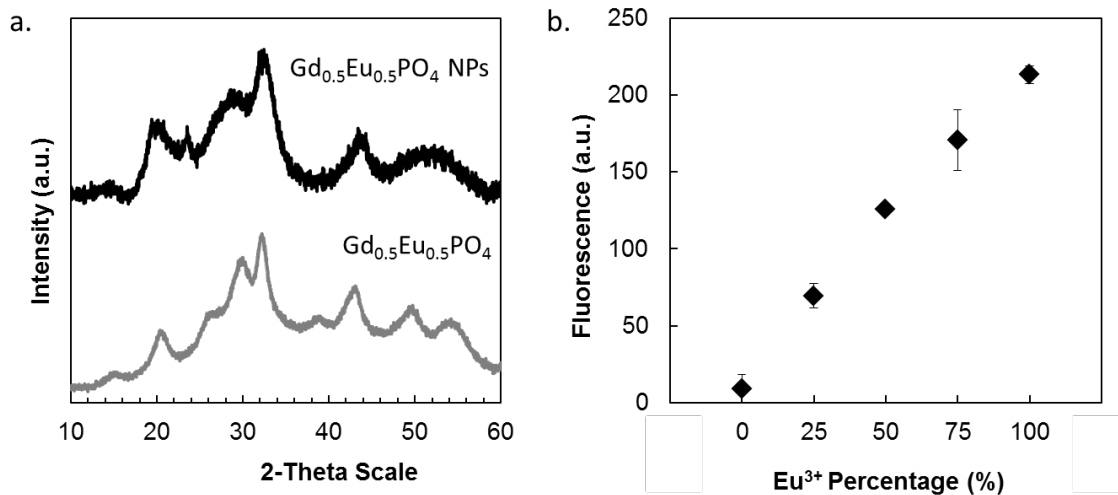


Figure S5. (a.) The XRD traces of the $Gd_{0.5}Eu_{0.5}PO_4$ nanoparticles and the $Gd_{0.5}Eu_{0.5}PO_4$ salt. The characteristic $Gd_{0.5}Eu_{0.5}PO_4$ peaks are observed. (b.) The fluorescence intensity of the nanoparticle can be controlled by modulating the Gd to Eu ratio. The intensity varies linearly with Eu content ($n=3$).

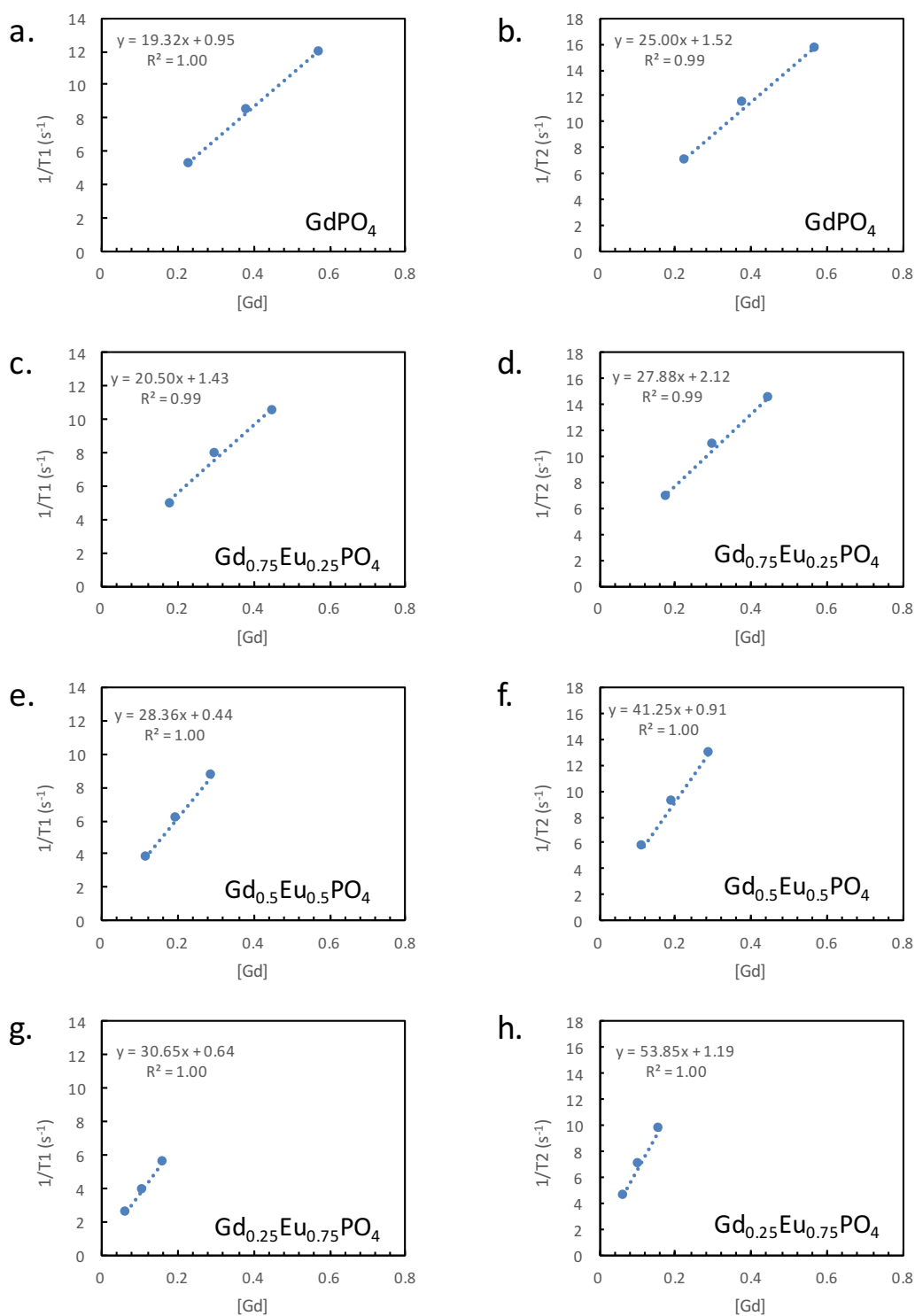


Figure S6. Plots of T_1 relaxation rates (column 1) and T_2 relaxation rates (column 2) as a function of gadolinium concentration for GdPO₄ nanoparticles with varying Gd to Eu ratios. (a-b) Gd/Eu 1/0, (c-d) Gd/Eu 0.75/0.25, (e-f) Gd/Eu 0.5/0.5 (g-h) Gd/Eu 0.25/0.75.

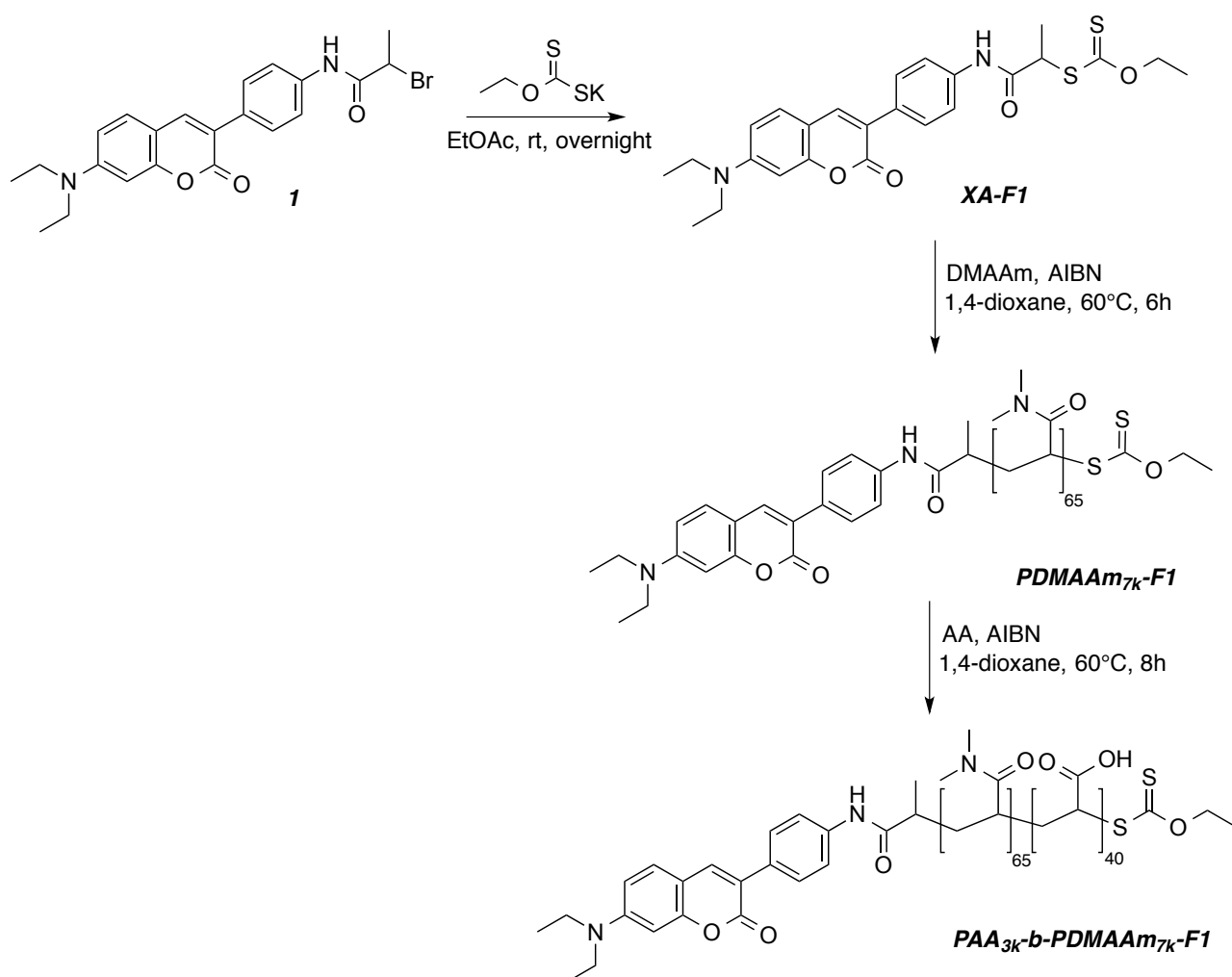
Polymer – Synthesis & Characterization

A. Homopolymer synthesis (PAA_{10K})

7 mg of 4,4'-Azobis(4-cyanovaleric acid) (ACVA), 43 mg of Rhodixan A1, 5 g of acrylic acid, 4 g of ethanol and 12.5 g of water were placed in a two-neck round-bottomed flask equipped with a magnetic stirrer and a reflux condenser. The solution was then degassed for 15 min by bubbling argon. It was then heated at 70 °C during four hours, keeping a slow stream of argon in the reactor. After this period of time, the solution was cooled down to ambient temperature and the polymer was analysed. AA conversion > 99% ($^1\text{H NMR}$ in D_2O). Dispersity values determined by size exclusion chromatography in water were found equal to 1.7.

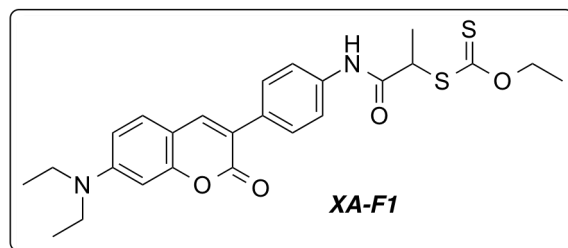
B. Fluorescent polymer synthesis ($PAA_{3K}\text{-}b\text{-}PDMAAm_{7K}\text{-}F1$)

The fluorescent block copolymer $PAA_{3K}\text{-}b\text{-}PDMAAm_{7K}\text{-}F1$ was synthesized in three steps from brominated coumarin **1** (**Scheme S1** below).



Scheme S1. Synthesis scheme of block copolymer $PAA_{3K}\text{-}b\text{-}PDMAAm_{7K}\text{-}F1$, starting from functionalized coumarin **1**.

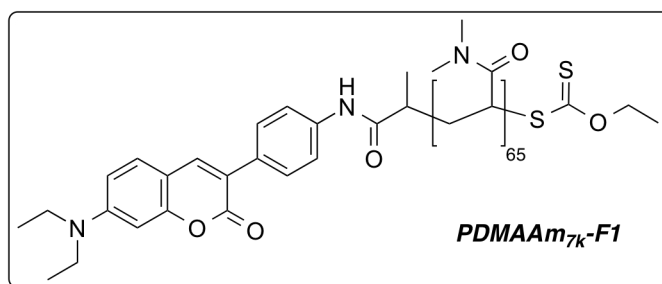
RAFT agent XA-F1 – In a dry flask were successively added under argon potassium *O*-ethyl xanthogenate (240 mg, 1.5 mmol), the functionalized coumarin **1**¹ (444 mg, 1 mmol) and dry ethyl acetate (5 mL) as solvent. After stirring overnight at room



temperature, the reaction mixture was diluted with 15 mL of DCM, filtered through celite and concentrated under reduced pressure. Purification of the resulting solid residue by column chromatography (elution with a dichloromethane/methanol 8:2 mixture), followed by recrystallization from ethanol/EtOAc, furnished **XA-F1** in pure form as an orange solid. – Yield 70% (340 mg). – FTIR-ATR (neat) 3327 (N-H), 1685 (C=O, coumarin), 1612 (C=O, amide), 1044 (C=S) cm⁻¹. – ¹H NMR (300 MHz, CDCl₃, 298 K): δ = 1.22 (t, ³J = 7.1 Hz, 6H), 1.43 (t, ³J = 7.1 Hz, 3H), 1.64 (d, ³J = 7.4 Hz, 3H), 3.42 (q, ³J = 7.1 Hz, 4H), 4.49 (q, ³J = 6.6 Hz, 1H), 4.68 (q, ³J = 7.1 Hz, 3H), 6.52 (d, ³J = 2.4 Hz, 1H), 6.59 (dd, ³J = 8.8 Hz, ⁴J = 2.5 Hz, 1H), 7.31 (d, ³J = 8.8 Hz, 1H), 7.56 (d, ³J = 8.8 Hz, 2H), 7.67 (s, 1H), 7.68 (d, ³J = 8.8 Hz, 2H), 8.42 (s, 1H, NH). – ¹³C NMR (75 MHz, CDCl₃, 298 K): δ = 12.6, 13.9, 16.2, 45.0, 48.5, 71.4, 97.2, 109.1, 109.3, 119.7, 120.2, 128.96, 129.03, 132.1, 137.3, 140.2, 150.6, 156.3, 161.8, 169.2, 214.5. – HRMS (ESI, 30 V, positive mode): *m/z*: calcd for C₂₅H₂₉N₂O₄S₂ 485.1569, found 485.1568, [MH]⁺.

Macro-RAFT agent PDMAAm_{7k}-F1 –

In a 15 mL Schlenk vacuum tube equipped with Rotaflo PTFE needle valve and a magnetic stir bar were successively added XA-F1 (242 mg, 0.5 mmol, 76.9 mmol L⁻¹), AIBN (8.2 mg,

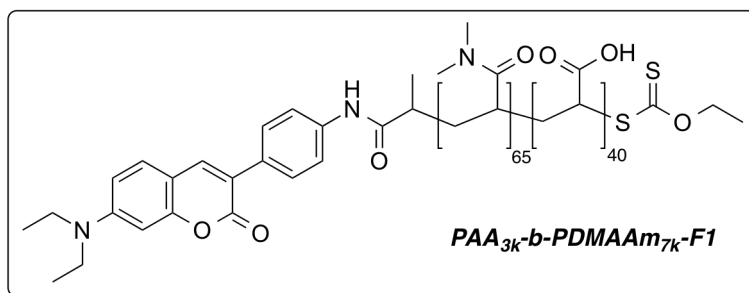


0.05 mmol, 7.69 mmol L⁻¹), DMAAm (3.22 g, 32.5 mmol, 5 mol L⁻¹) and 1,4-dioxane (3.15 mL) as solvent. After degassing with five freeze-pump-thaw cycles, the reaction mixture was sealed under vacuum and after 6 hours heating at 60°C in an aluminium heating block (reaching 99% monomer conversion), the resulting polymer was isolated by rotary evaporation and freeze dried. – Recovery 3.2 g (92 %). – *M_n* = 7.24 kDa. – *Đ* = 1.09 (dn/dc = 0.148 mL g⁻¹).

Block copolymer PAA_{3k}-b-**PDMAAm_{7k}-F1**

In a 15 mL Schlenk vacuum tube equipped with Rotaflo PTFE needle valve and a magnetic stir bar were successively added added

PDMAAm_{7k}-F1 macro-RAFT agent (2.1 g, 0.3 mmol, 30 mmol L⁻¹), AIBN (4.9 mg, 0.03 mmol, 3 mmol L⁻¹), AA (1.08 g, 15 mmol, 2.5 mol L⁻¹) and 1,4-dioxane (2.9 mL) as solvent. After degassing with five freeze-pump-thaw cycles reaction mixture was sealed under vacuum and after 8 hours heating at 60°C in an aluminium heating block (reaching 80% monomer conversion), the resulting polymer was isolated by rotary evaporation and freeze dried. – Recovery 2.8 g (94 %). – $M_n = 10.2$ kDa. – $D = 1.11$ (dn/dc = 0.0904 mL g⁻¹).



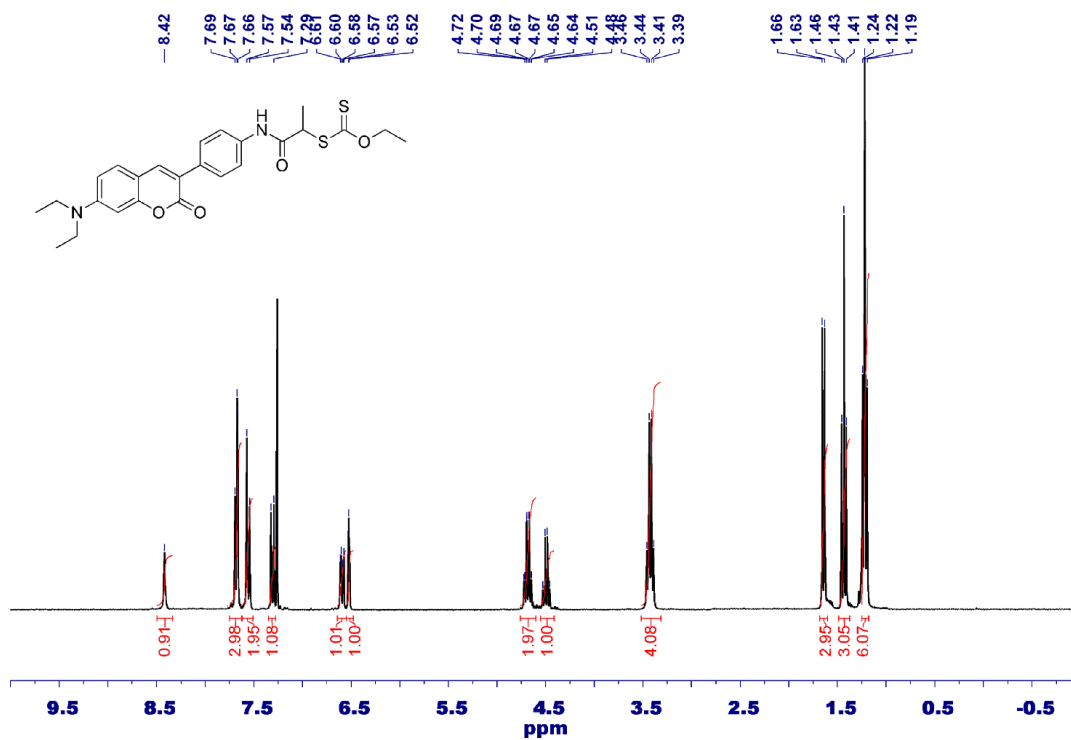


Figure S7. ¹H NMR spectrum (300 MHz, CDCl₃) of RAFT agent XA-F1.

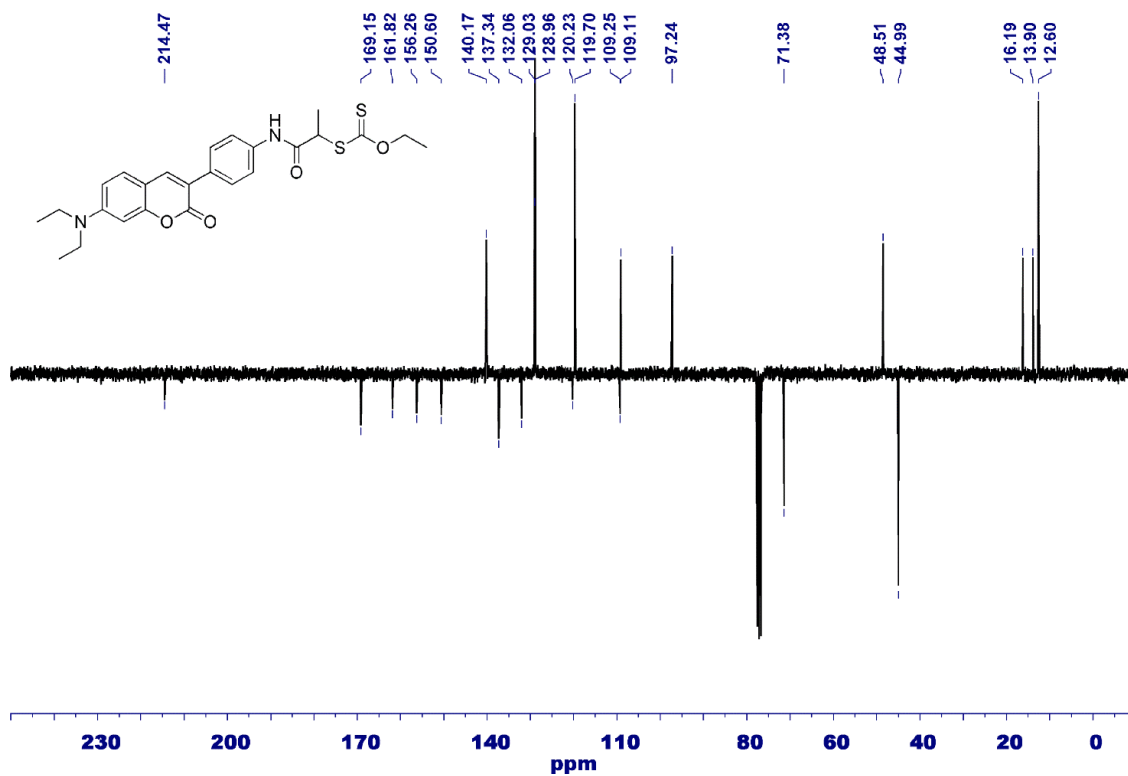


Figure S8. ¹³C NMR spectrum (75 MHz, CDCl₃) of RAFT agent XA-F1.

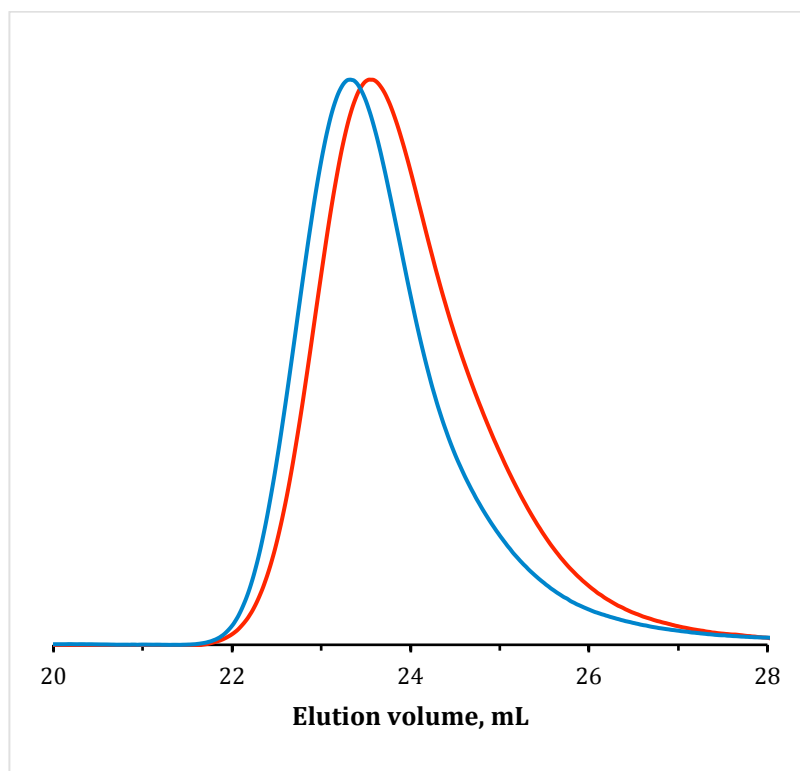
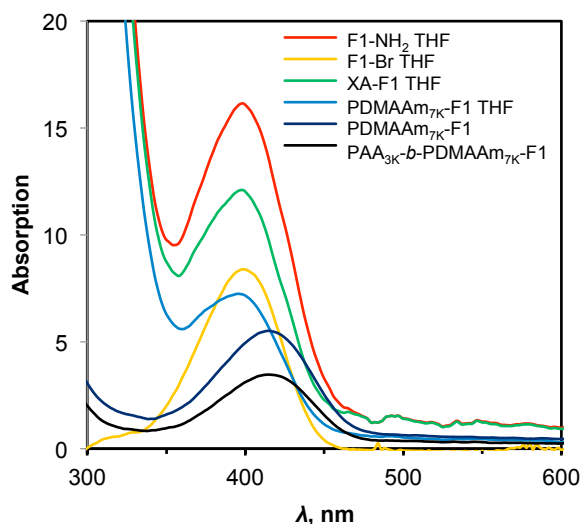
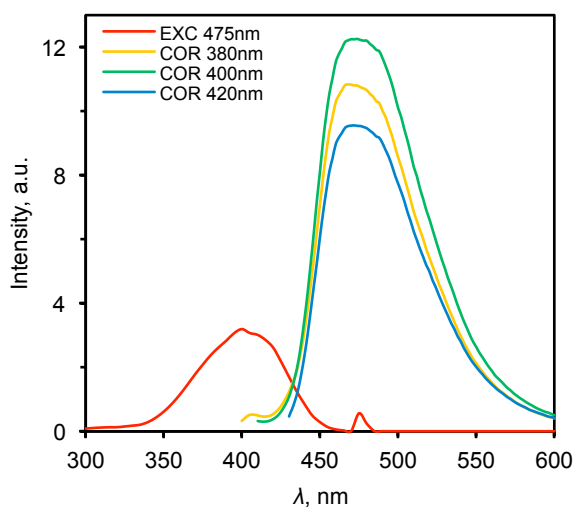


Figure S9. SEC traces of PDMAAm_{7k}-F1 (red) and PAA_{3k}-*b*-PDMAAm_{7k}-F1 (blue).

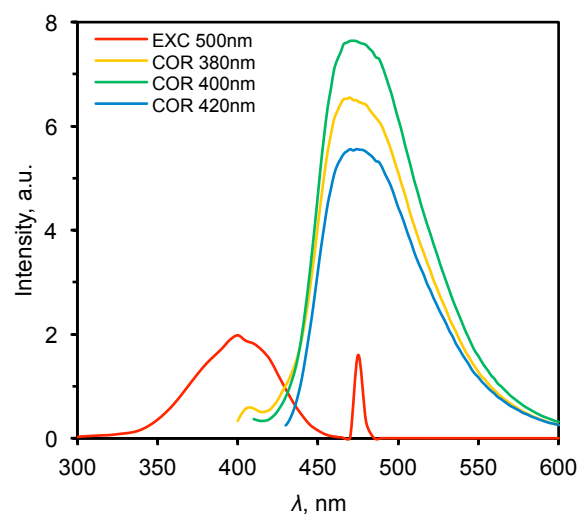
Figure S10. a) UV-vis spectra of the different species bearing the coumarin moiety (see Scheme S1) and b) c) d) e) Emission spectra of the different species at three different excitation wavelength (λ_{ex} = 380, 400 or 420 nm) and excitation spectrum at an emission wavelength of 500 nm.



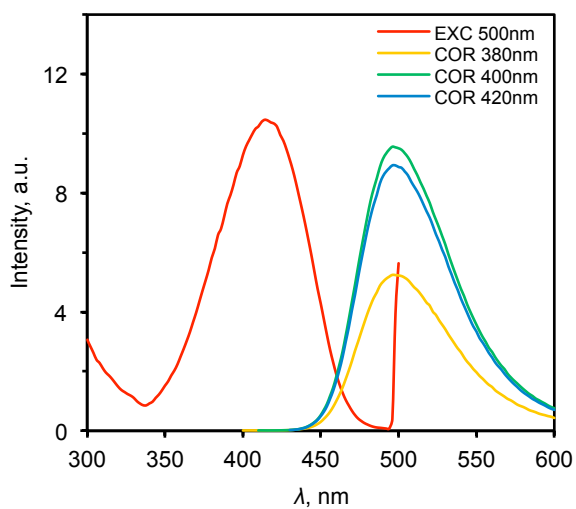
a) UV-vis spectra



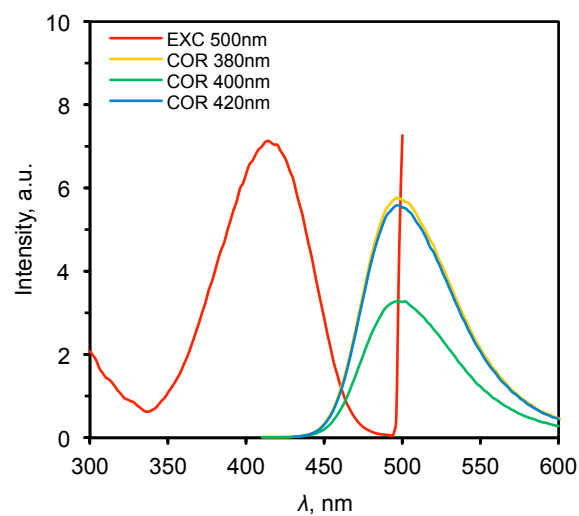
b) XA-F1 in THF



c) PDMAAm_{7k}-F1 in THF



d) PDMAAm_{7k}-F1 in water



e) PAA_{3k}-b-PDMAAm_{7k}-F1 in water

PEGylated Fluorescent Nanoparticle Characterization

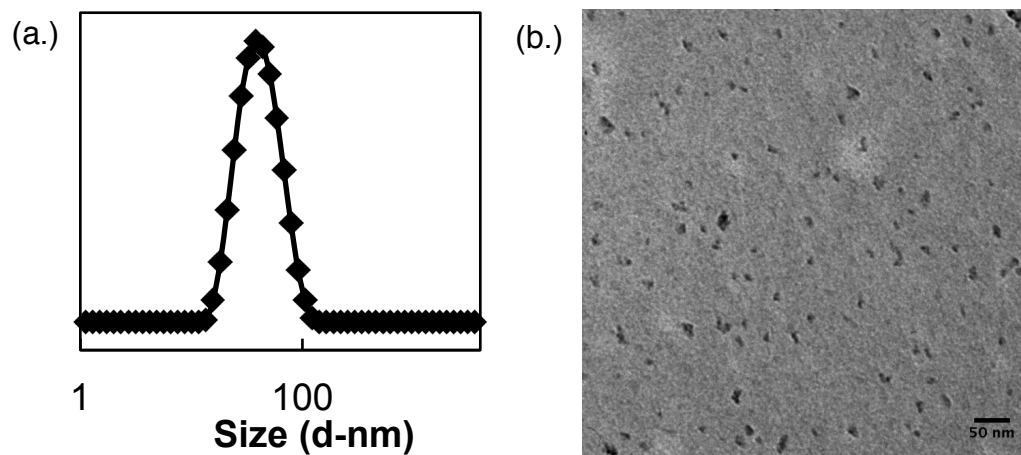


Figure S11. (a.) Intensity weighted hydrodynamic diameter distribution of GdPO_4 nanoparticles coated with a 4:1 wt/wt mixture of PAA-PEG and PAA-PDMAAm-F1 (after purification by centrifugation). The particles have an average size of 44 nm (PDI = 0.16). (b.) TEM image of GdPO_4 NPs nanoparticles coated with a 4:1 wt/wt mixture of PAA-PEG and PAA-PDMAAm-F1.

References

1. I. Kulai, S. Mallet-Ladeira, *J. Mol. Struct.*, **2016**, *1104*, 14.
2. J. Han, Z. Zhu, H. Qian, A. R. Wohl, C. J. Beaman, T. R. Hoye, C. W. Macosko, *J. Pharm. Sci.* **2012**, *10*, 4018.